units bridged by a difunctional diphos ligand.[39]

The ^{31}P NMR spectrum of bis-substituted E consists of a well-resolved 1:2:1 triplet at δ 283.4 for the two phosphinidene caps and another well-resolved 1:2:1 triplet at δ 66.7 for the two coordinated phosphine ligands, with both triplets of equal intensity. The mass spectrometric determination of the molecular weight of *m/e* 986 precludes a dimeric structure for E. The ligand can be bis-coordinated to the triiron cluster in three possible ways, i.e., diphos chelating the Fe(1) center, bridging the Fe(1) and Fe(2) centers, or bridging the Fe(1) and Fe(3) centers, which we designate as isomers a, b, and c, respectively. Isomer b can be rejected on the basis of the observed triplet splitting at δ 66.7, which indicates the presence of two equivalent phosphine ligand centers on E. [Note that phosphine ligands and Fe(1) and Fe(2) on triiron clusters cannot be accidentally degenerate (see Table V). Isomer a consists of diphos in a 5-membered ring, whereas isomer c has it in a quasi-6-membered ring. Garrou[35,40] has shown that the phosphorus coordination to a metal in a 5-membered chelate ring is highly shielded. Thus, the ring effect parameter, $\Delta_r = \delta(L_{coord}) - \delta(L_{free})$, is large and positive for 5-membered rings, highly negative for 4-membered rings, and close to zero or weakly negative for 6-membered rings. Evaluated in this way, triiron cluster E with $\Delta_r = +3.7$ is the 6-membered isomer c. Although we were able to grow a single crystal of E as a fine dark red needle, it was unfortunately not suitable for X-ray crystallography. Barring our extensive efforts to grow another crystal modification, we rely on the ^{31}P NMR spectral analysis for the structural assignment of E.

ESR Spectroscopy. Solutions of the closed anion radicals (Table III) were prepared by reduction of the triiron cluster with 1% sodium amalgam in tetrahydrofuran or acetonitrile. The reduction of $Fe_3(PPh)_2(CO)_9$ (A) by cobaltocene in acetonitrile also afforded the closed anion radical $A^{-}\cdot$. The ESR spectrum of $A^{-}\cdot$ shown in Figure 3a is essentially the same as that obtained in THF by the sodium amalgam reduction (vide supra). Upon standing, $A^{-}\cdot$ rearranges to open species $A_i^{-}\cdot$ showing the ESR spectrum in Figure 2a. The substituted derivatives $C_i^{-}\cdot$ presented in Table I were generated in situ by the addition of the appropriate phosphine. The same ESR spectra were obtained by the sodium amalgam reduction of the triiron cluster $Fe_3(PPh)_2(CO)_8L$ in acetonitrile and by allowing the solution to stand. The solutions of the anion radicals were transferred with the aid of a hypodermic syringe into ESR tubes that were then sealed in vacuo. For the description of the ESR technique, see ref 41.

Acknowledgment. We thank the National Science Foundation and the Robert A. Welch Foundation for financial support. H. H. Ohst is a recipient of a NATO grant administered under the auspices of the German Academic Exchange Service.

Registry No. A, 38903-71-8; A^{-}, 101198-33-8; A^{2-}, 102000-25-9; A_i^{-}, 101011-28-3; AH^{-}, 102046-68-4; AH'^{-}, 102000-51-1; AMe^{-}, 102046-69-5; B (isomer I), 101011-19-2; B (isomer II), 102000-28-2; C (L = $P(OMe)_3$, isomer I), 39040-36-3; C (L = $P(OMe)_3$, isomer II), 102000-29-3; C (L = PPh_3), 102130-35-8; $C^{-}\cdot$ (L = PEt_3), 101011-27-2; $C^{-}\cdot$ (L = $P(OMe)_3$), 101011-23-8; $C^{-}\cdot$ (L = PPh_3), 101011-22-7; $C_i^{-}\cdot$ (L = PPh_3), 101011-24-9; $C_i^{-}\cdot$ (L = $P(p\text{-}ClC_6H_4)_3$), 102000-35-1; $C_i^{-}\cdot$ (L = $P(p\text{-}MeC_6H_4)_3$), 102046-67-3; $C_i^{-}\cdot$ (L = $P(p\text{-}MeOC_6H_4)_3$), 102000-36-2; $C_i^{-}\cdot$ (L = PPh_2Et), 102000-38-4; $C_i^{-}\cdot$ (L = PPh_2Me), 102000-39-5; $C_i^{-}\cdot$ (L = $PPhEt_2$), 102000-40-8; $C_i^{-}\cdot$ (L = $PPhMe_2$), 102000-41-9; $C_i^{-}\cdot$ (L = PEt_3), 101011-25-0; $C_i^{-}\cdot$ (L = $P(i\text{-}Pr)_3$), 102000-42-0; $C_i^{-}\cdot$ (L = PBu_3), 102000-43-1; $C_i^{-}\cdot$ (L = $P(c\text{-}C_6H_{11})_3$), 102000-44-2; $C_i^{-}\cdot$ (L = $PPh_2(OBu)$), 102000-45-3; $C_i^{-}\cdot$ (L = $PPh(OBu)_2$), 102000-46-4; $C_i^{-}\cdot$ (L = $P(OPh)_3$), 102000-47-5; $C_i^{-}\cdot$ (L = $P(OMe)_3$), 102000-48-6; $C_i^{-}\cdot$ (L = $P(O\text{-}i\text{-}Pr)_3$), 102000-49-7; $C_i^{-}\cdot$ (L = $AsPh_3$), 102000-50-0; D (isomer I), 102000-26-0; D^{-} (isomer I), 102000-32-8; $D^{-}\cdot$ (isomer II), 102000-33-9; $D_i^{-}\cdot$ (isomer I), 102000-37-3; E (isomer IV), 102000-27-1; $E^{-}\cdot$ (isomer IV), 102000-34-0; $Fe_3(PPh)_2(CO)_7[P(OMe)_3]_2$ (isomer III), 102000-30-6; $Fe_3(PPh)_2(CO)_7[P(OMe)_3]_2$ (isomer IV), 102000-31-7; $Fe_3(PPh)_2(CO)_7(PEt_3)_2$ (isomer III), 102046-70-8; CH_3CO_2H, 64-19-7; Fe, 7439-89-6; P, 7723-14-0.

(39) Cunninghame, R. G.; Downard, A. J.; Hanton, L. R.; Jensen, S. D.; Robinson, B. H.; Simpson, J. *Organometallics* **1984**, *3*, 180.
(40) Garrou, P. E. *Inorg. Chem.* **1975**, *14*, 1435.
(41) Lau, W.; Huffman, J. C.; Kochi, J. K. *Organometallics* **1982**, *1*, 155.

Contribution from the Department of Chemistry, The University of Houston, University Park, Houston, Texas 77004

Electrochemistry of $Mn_2(CO)_{10}$, $[Mn(CO)_5]^+$, $[Mn(CO)_5]^-$, and $Mn(CO)_5$

D. A. Lacombe, J. E. Anderson, and K. M. Kadish*

Received November 4, 1985

A self-consistent electrochemical mechanism for the reduction and oxidation of the $Mn_2(CO)_{10}$ metal–metal bonded dimer, and the associated monomeric $[Mn(CO)_5]^+$ and $[Mn(CO)_5]^-$ ions, was determined by the use of various electrochemical methods. The dimer is both reduced and oxidized by an overall two electrons with the initial step being the formation of the monomeric 17-electron $Mn(CO)_5$ radical. This radical was shown to be a key intermediate species in all of the electrochemical oxidations and reductions. It was also shown that the $[Mn(CO)_5]^-$ and $[Mn(CO)_5]^+$ ions could be directly interconverted via an overall two-electron-transfer sequence that passed through the $Mn(CO)_5$ species. This type of reactivity has not previously been reported.

Introduction

The electrochemistry of organometallic metal–metal bonded complexes has been the object of many studies over the last 20 years.[1-10] Numerous dimers of the form M_2L_2 have been examined where M is a metal or metalate ion and L is the set of ligands of the form $(CO)_x(\eta^5\text{-}C_5H_5)_y$. Perhaps the most studied complex of this type is $Mn_2(CO)_{10}$. This complex may be oxidized in nonaqueous media by two electrons[4] to yield $[Mn(CO)_5]^+$, or the dimer may be reduced by two electrons[1-4,11-13] to yield $[Mn(CO)_5]^-$. The 17-electron $Mn(CO)_5$ radical may also be photochemically generated from $Mn_2(CO)_{10}$, and the characterization and reactivity of this radical has been the object of numerous studies.[14-28]

(1) Dessy, R. E.; Stary, F. E.; King, R. B.; Waldrop, W. *J. Am. Chem. Soc.* **1966**, *88*, 471.
(2) Dessy, R. E.; Weissman, P. M.; Pohl, R. L. *J. Am. Chem. Soc.* **1966**, *88*, 5117.
(3) Lemoine, P.; Giraudeau, A.; Gross, M. *Electrochim. Acta* **1976**, *21*, 1.
(4) Pickett, C. J.; Pletcher, D. *J. Chem. Soc., Dalton Trans.* **1975**, 879.
(5) Denisovitch, L. I.; Gubin, S. P.; Chapovskii, Y. A.; Ustynok, N. A. *Bull. Acad. Sci. USSR, Div. Chem. Sci. (Engl. Transl.)* **1971**, *20*, 1851.
(6) Madach, T.; Vahrenkamp, H. *Z. Naturforsch., B: Anorg. Chem., Org. Chem.* **1979**, *34B*, 573.
(7) Ferguson, J. A.; Meyer, T. J. *Inorg. Chem.* **1971**, *10*, 1025.
(8) Miholova, D.; Vlcek, A. A. *Inorg. Chim. Acta* **1980**, *41*, 119.
(9) de Montauzon, D.; Poilblanc, R.; Lemoine, P.; Gross, M. *Electrochim. Acta* **1978**, *23*, 1247.
(10) Connelly, N. G.; Geiger, W. E. *Adv. Organomet. Chem.* **1984**, *23*, 1.
(11) Colton, R.; Dalziel, J.; Griffith, W. P.; Wilkinson, G. *J. Chem. Soc.* **1960**, 71.
(12) Denisovich, L. I.; Ioganson, A. A.; Gubin, S. P.; Kolobova, N. E.; Anisimov, K. N. *Bull. Acad. Sci. USSR, Div. Chem. Sci. (Engl. Transl.)* **1969**, *18*, 218.
(13) Lemoine, P.; Gross, M. *J. Organomet. Chem.* **1977**, *133*, 193.
(14) Walker, H. W.; Herrick, R. S.; Olsen, R. J.; Brown, T. L. *Inorg. Chem.* **1984**, *23*, 3748.
(15) Wagman, R. W.; Olsen, R. J.; Gard, D. R.; Faulkner, L. R.; Brown, T. L. *J. Am. Chem. Soc.* **1981**, *103*, 6089.
(16) Hughey, J. L.; Anderson, C. P.; Meyer, T. J. *J. Organomet. Chem.* **1977**, *125*, C49.

0020-1669/86/1325-2074$01.50/0

The electroreduction and electrooxidation of $Mn_2(CO)_{10}$ involves irreversible two-electron-transfer reactions as shown in eq 1 and 2. These reactions are diffusion-controlled and give

$$Mn_2(CO)_{10} + 2e^- \rightarrow 2[Mn(CO)_5]^- \quad (1)$$

$$Mn_2(CO)_{10} \rightarrow 2[Mn(CO)_5]^+ + 2e^- \quad (2)$$

well-defined voltammograms in nonaqueous media. It is known that the initial electroreduction of $Mn_2(CO)_{10}$ involves a rate-controlling (slow) electron-transfer step,[3] but a self-consistent, detailed electrochemical mechanism for the reduction and oxidation of $Mn_2(CO)_{10}$, $[Mn(CO)_5]^-$, and $[Mn(CO)_5]^+$ has not been reported.

In this study, we have reexamined the electroreduction and electrooxidation mechanisms of $Mn_2(CO)_{10}$ and have intercompared the results for this compound with those of $[Mn(CO)_5]^+$, $[Mn(CO)_5]^-$, and the $Mn(CO)_5$ radical. This was done in both bonding and nonbonding solvents. From these data we have developed an overall oxidation and reduction scheme for all of these species. In addition to the interconversions previously reported for these compounds, we have shown that $[Mn(CO)_5]^+$ can be directly generated from $[Mn(CO)_5]^-$ and that $[Mn(CO)_5]^-$ can be directly generated from $[Mn(CO)_5]^+$. We have also shown that the electrochemical reactions of $Mn_2(CO)_{10}$ invariably proceed via the $Mn(CO)_5$ radical intermediate and that $Mn(CO)_5$ is the key species in all of the electrochemistry.

Experimental Section

Instrumentation. All electrochemical measurements were performed with a BAS 100 electrochemical analyzer connected to a Houston Instruments HIPLOT DMP-40 plotter. Cyclic voltammetry, linear-sweep voltammetry, and voltammetry at a rotating Pt-disk electrode (area 1.95 mm^2) were all utilized. Scan rates between 50 mV/s and 50 V/s were utilized for the first two techniques while for rotating-disk voltammetry the rotation rate was varied between 1500 and 5000 rpm.

A three-electrode system was used for all measurements. This consisted of a Pt-button working electrode (area 0.7 mm^2), a Pt-wire counter electrode, and a silver-wire pseudoreference electrode. This electrode was separated from the bulk of the solution by a fritted-glass bridge containing the supporting electrolyte and solvent. Potentials of the Fc^+/Fc couple were also measured with this electrode, and values of $E_{1/2}$ for each complex are then reported vs. a saturated calomel electrode (SCE) after correction with ferrocene. In several cases, potentials were also measured directly vs. a commercial SCE. These values were also referenced vs. the Fc^+/Fc couple.

All voltammetric experiments were carried out in a Vacuum Atmospheres drybox under a nitrogen atmosphere. The compounds were also stored in the drybox. Solutions contained 0.1 M tetrabutylammonium perchlorate (TBAP) as supporting electrolyte for all of the electrochemical experiments. All solvents were degassed with a stream of Linde prepurified argon for 10 min directly after distillation and before being introduced into the drybox. Experiments were run in the dark and in the light to test the photoactivity of the compound. The results of the experiments run in the dark were similar to those obtained in the light so that no special precautions were taken with respect to light.

Chemicals. Tetrabutylammonium perchlorate (TBAP) was purchased from Fluka and purified by recrystallization from a 20:80 mixture of hexane and ethyl acetate. All solvents were purified as described below and stored under nitrogen and were then freshly distilled before use. Reagent grade methylene chloride (CH_2Cl_2) was distilled from CaH_2. Tetrahydrofuran (THF) was distilled under argon from a mixture of sodium and benzophenone. HPLC grade acetonitrile (CH_3CN) was refluxed for 1 h from $KMnO_4$, followed by distillation.

$Mn_2(CO)_{10}$ was purchased from either Alfa or Aldrich and used without further purification. The sodium salt of the monoanion was prepared by reduction of the corresponding dimer with a sodium amalgam in THF. The monocation was prepared in situ by electrochemical oxidation of the corresponding dimer. Both $Mn_2(CO)_{10}$ and $Na[Mn(CO)_5]$ were stored in the drybox under an inert N_2 atmosphere.

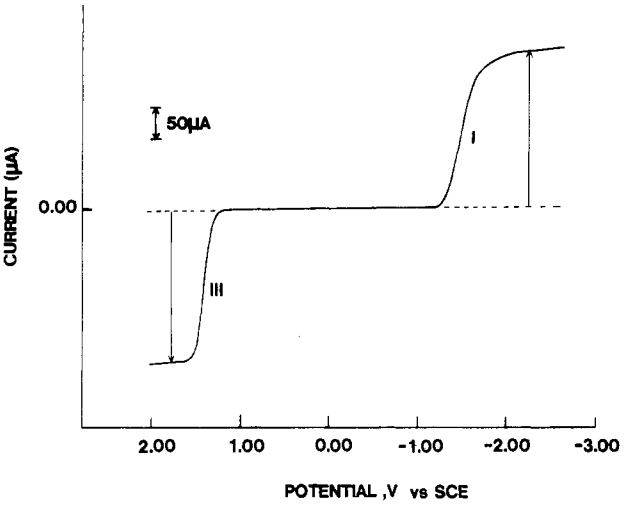

Figure 1. Voltammogram of $Mn_2(CO)_{10}$ at a Pt rotating-disk electrode in CH_3CN (0.1 M TBAP). The rotation rate was 5000 rpm and the potential scan rate = 0.4 V/s.

Table I. Cyclic Voltammetric Peak Potentials (V vs. SCE) for Oxidation and Reduction of Various Dimeric, Anionic, and Cationic Species of $Mn_2(CO)_{10}$ in Three Solvents Containing 0.1 M TBAP[a]

	$Mn_2(CO)_{10}$		$[Mn(CO)_5]^-$	$[Mn(CO)_5]^+$
solvent	redn	oxidn	oxidn	redn
CH_2Cl_2	−1.49	1.55	−0.19	−0.76
THF	−1.32		−0.06	
CH_3CN	−1.45	1.35	−0.12	−1.10

[a] All values were obtained at a scan rate of 0.2 V/s and were measured by using an Ag-wire pseudoreference electrode.

Results and Discussion

Electrochemistry of $Mn_2(CO)_{10}$ and $[Mn(CO)_5]^-$. Figure 1 illustrates the voltammogram of $Mn_2(CO)_{10}$ at a rotating Pt-disk electrode in CH_3CN (0.1 M TBAP). The single reduction wave of $Mn_2(CO)_{10}$ is labeled process I while the oxidation wave is labeled process III. Values of $E_{1/2}$ for each of these processes depend upon the rotation rate, and at a rotation of 5000 rpm values of $E_{1/2}$ = −1.41 and 1.33 V were obtained.

Potentials for the global two-electron reduction of $Mn_2(CO)_{10}$ vary substantially as a function of solvent and supporting electrolyte and have been reported to occur at −1.8 V vs. $Ag/AgClO_4$ in dimethoxyethane containing 0.1 M TBAP,[1,2] at −1.65 V vs. SCE in THF containing 0.2 M (TBA)PF_6 (0.3 V/s),[4] at −1.15 V vs. SCE in C_2H_5OH containing 0.3 M (TMA)Cl,[11] and at −1.06 V vs. SCE in propylene carbonate containing 0.05 M (TEA)Br.[3] In this study, values of E_p for the electroreduction varied between −1.32 V (THF) and −1.49 V (CH_2Cl_2) by cyclic voltammetry when the scan rate was 0.2 V/s and the solvent contained 0.1 M TBAP. These values are listed in Table I, which also gives values of E_p in CH_3CN.

The electroreduction of $Mn_2(CO)_{10}$ may proceed via the singly reduced $[Mn_2(CO)_{10}]^-$ radical (reaction 3), but this anionic species has not been identified in any electrochemical study. On the other

$$Mn_2(CO)_{10} + e^- \rightleftarrows [Mn_2(CO)_{10}]^- \quad (3)$$

hand, the formation of a $[Mn_2(CO)_{10}]^-$ radical has been suggested

(17) Huffadine, A. S.; Peake, B. M.; Robinson, B. H.; Simpson, J.; Dawson, P. A. *J. Organomet. Chem.* **1976**, *12*, 391.
(18) Lindsell, W. E.; Preston, P. N. *J. Chem. Soc., Dalton Trans.* **1979**, 1105.
(19) Hepp, A. F.; Wrighton, M. S. *J. Am. Chem. Soc.* **1981**, *103*, 1258.
(20) Abrahamson, H. B.; Wrighton, M. S. *J. Am. Chem. Soc.* **1977**, *99*, 5510.
(21) Wrighton, M. S.; Ginley, D. S. *J. Am. Chem. Soc.* **1975**, *97*, 2065.
(22) Freedman, A.; Bersohn, R. *J. Am. Chem. Soc.* **1978**, *100*, 4116.
(23) Fox, A.; Poe, A. *J. Am. Chem. Soc.* **1980**, *102*, 2498.
(24) Yosaka, H.; Kobayashi, T.; Yasufuku, K.; Nagakura, S. *J. Am. Chem. Soc.* **1983**, *105*, 6249.
(25) Rothberg, L. J.; Cooper, N. J.; Peters, K. S.; Vaida, V. *J. Am. Chem. Soc.* **1982**, *104*, 3536.
(26) Stiegman, A. E.; Tyler, D. R. *Inorg. Chem.* **1984**, *23*, 527.
(27) Kidd, D. R.; Brown, T. L. *J. Am. Chem. Soc.* **1978**, *100*, 4095.
(28) Hudson, A.; Lappert, M. F.; Nicholson, B. K. *J. Chem. Soc., Dalton Trans.* **1977**, 551.

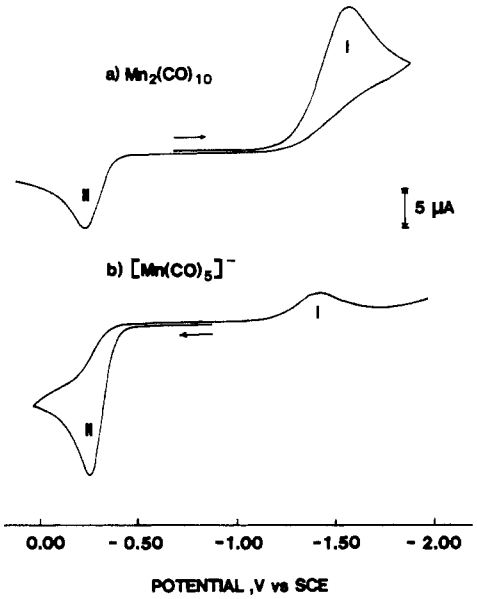

Figure 2. Cyclic voltammogram of (a) $Mn_2(CO)_{10}$ in CH_2Cl_2 (0.1 M TBAP) and (b) $[Mn(CO)_5]^-$ in CH_2Cl_2 (0.1 M TBAP). This later anionic species was generated from $Mn_2(CO)_{10}$ by controlled-potential reduction at −1.7 V vs. SCE. Voltammograms were obtained at a scan rate of 0.2 V/s.

by ESR studies on irradiated solids of $Mn_2(CO)_{10}$ that were carried out at 77 K.[29] However, later studies have suggested that $[Mn_2(CO)_9]^-$ was actually formed[30] by irradiation of the $Mn_2(CO)_{10}$ solid.

The proposed formation of $[Mn_2(CO)_{10}]^-$ by pulse radiolysis in ethanol leads to a rapid cleavage of the Mn–Mn bond, giving $[Mn(CO)_5]^-$ and $Mn(CO)_5$ as shown in eq 4.[31] The generated

$$[Mn_2(CO)_{10}]^- \xrightarrow{\text{fast}} [Mn(CO)_5]^- + Mn(CO)_5 \qquad (4)$$

$Mn(CO)_5$ radical is electroreducible at the potential of $Mn_2(CO)_{10}$ reduction, and the rapid addition of one electron to this species leads to a second molecule of $[Mn(CO)_5]^-$, thus giving the overall two-electron reduction shown in eq 1.

A cyclic voltammogram for the reduction and reoxidation of $Mn_2(CO)_{10}$ in CH_2Cl_2 containing 0.1 M TBAP is shown in Figure 2. A single reduction and a single oxidation peak are observed in the range of potentials between 0.00 and −2.00 V vs. SCE. The exact potentials for these reactions were dependent upon scan rate and also upon whether $Mn_2(CO)_{10}$ was in the bulk of solution or was generated from $[Mn(CO)_5]^-$. For example, the reduction peak (process I) occurs at −1.49 V in Figure 2a (which contains bulk $Mn_2(CO)_{10}$) and at −1.40 V in Figure 2b (which contains bulk $[Mn(CO)_5]^-$). At the same time the oxidation peak (process II) is located at −0.19 V in Figure 2a and at −0.21 V in Figure 2b. These differences in potentials were always observed after bulk electrolysis of $Mn_2(CO)_{10}$.

A peak for process II is not present if the initial negative potential sweep is stopped before −1.40 V, and thus peak II is clearly due to the oxidation of $[Mn(CO)_5]^-$, as reported by both Lemoine[3] and Pletcher.[4] In this study, a reversible reduction peak I was never observed, even at temperatures as low as −75 °C and at scan rates as high as 50 V/s. This suggests either an irreversible (rate-controlling) electron-transfer step or a coupled chemical reaction that follows the electron transfer in CH_2Cl_2 and is too fast to be observed on the cyclic voltammetric time scale. According to Lemoine,[3] the reduction of $Mn_2(CO)_{10}$ is electrochemically irreversible in propylene carbonate and an $\alpha n = 0.37 \pm 0.07$ can be calculated for the initial step in the rate-determining two-electron reduction.

Table II. Values of $|E_p - E_{p/2}|$ (±5 mV) for Reduction and Oxidation of Various Dimeric, Anionic, and Cationic $Mn_2(CO)_{10}$ Species

	$Mn_2(CO)_{10}$		$[Mn(CO)_5]^-$	$[Mn(CO)_5]^+$
solvent	redn	oxidn	oxidn	redn
CH_2Cl_2	112	55	61	112
THF	113	...	64	
CH_3CN	136	59	59	94

Table III. Transfer Coefficients, αn, for Reduction of $Mn_2(CO)_{10}$ in Various Solvents[a]

	parameter		
solvent	$E_p - E_{p/2}$	$\Delta E_p/\Delta \log V$	$\Delta E/\Delta \log (i/(i_d - i))$
CH_2Cl_2	0.53	0.45	...
THF	0.52	0.47	
CH_3CN	0.43	...	0.40
PC	...	...	0.37[b]

[a] Values of α given to ±0.05. [b] Reference 3 (value given to ±0.07).

Our results and interpretations in CH_2Cl_2 are consistent with those in propylene carbonate. Analysis of the $Mn_2(CO)_{10}$ reduction in CH_2Cl_2 was accomplished with the criteria of Savéant and Vianello,[32,33] which are similar to those of Nicholson and Shain.[34,35] As seen in Figure 2a the shape of the reduction peak is broader than that expected for either a one- or a two-electron-transfer, diffusion-controlled process (which would have $|E_p - E_{p/2}|$ values of 60 and 30 mV, respectively). The experimentally observed $|E_p - E_{p/2}|$ value for process I is 112 ± 5 mV in CH_2Cl_2 and is independent of scan rate. This peak separation is listed in Table II and can only be consistent with a rate-controlling (slow) electron transfer for which a transfer coefficient, αn, of 0.53 ± 0.05 is calculated. The peak potential dependence on scan rate also indicates an initial rate-controlling electron-transfer step. Values of $\Delta E_p/\Delta \log V$ were equal to 67 mV. This gives $\alpha n = 0.45 \pm 0.05$, a value which is within experimental error of that calculated from the peak shape. It is also in agreement with $\alpha n = 0.37 \pm 0.07$ calculated by Lemoine[3] for reduction of the same complex in propylene carbonate (see Table III).

Diagnostic criteria have been published for evaluating cyclic voltammetric curves that are characteristic of coupled chemical and electrochemical reactions.[32-35] The addition of one electron followed first by an irreversible chemical reaction and then by a second one-electron transfer is the classic case of an electrochemical ECE mechanism. Currents for a reduction mechanism of this type may depend upon the potential sweep rate, and in the limiting case (where the chemical reaction is the rate-determining step) the peak potential, E_p, will shift by 30 mV/10-fold change in sweep rate.[34] Unfortunately, an ECE mechanism where the first electron-transfer step is irreversible will give peak potential shifts that are determined not by the chemical reaction rate but by the rate-determining electron-transfer step.[35] Thus, the experimental data cannot rule out an EEC electrochemical reduction mechanism that is given by the reaction sequence (5a)–(5c).

$$Mn_2(CO)_{10} + e^- \xrightarrow{\text{rate determining}} [Mn_2(CO)_{10}]^- \qquad (5a)$$

$$[Mn_2(CO)_{10}]^- + e^- \rightleftarrows [Mn_2(CO)_{10}]^{2-} \qquad (5b)$$

$$[Mn_2(CO)_{10}]^{2-} \rightarrow 2[Mn(CO)_5]^- \qquad (5c)$$

On the other hand, results from the literature[29-31] on the stability of $[Mn_2(CO)_{10}]^-$ suggest that the formation of $[Mn_2(CO)_{10}]^{2-}$ is even less likely, and this strongly suggests that the electro-

(29) (a) Anderson, O. P.; Symons, M. C. R. *J. Chem. Soc., Chem. Commun.* **1972**, *1021*. (b) Bratt, S. W.; Symons, M. C. R. *J. Chem. Soc., Dalton Trans.* **1977**, 1314.
(30) Lionel, T.; Morton, J. R.; Preston, K. F. *Inorg. Chem.* **1983**, *22*, 145.
(31) Waltz, W. L.; Hackelberg, O. H.; Dorfman, L. M.; Wojcicki, A. *J. Am. Chem. Soc.* **1978**, *100*, 7259.
(32) Savéant, J.-M.; Vianello, E. *Electrochim. Acta* **1963**, *8*, 905.
(33) Savéant, J.-M.; Vianello, E. *Electrochim. Acta* **1967**, *12*, 1545.
(34) Nicholson, R. S.; Shain, I. *Anal. Chem.* **1964**, *36*, 706.
(35) Nicholson, R. S.; Shain, I. *Anal. Chem.* **1965**, *37*, 178.

chemical reduction of $Mn_2(CO)_{10}$ proceeds via an ECE and not an EEC type mechanism. An alternate sequence of steps involving initial cleavage of the metal–metal bond before electroreduction (a CE mechanism) might also be envisioned, but this mechanism can be ruled out on the basis of the experimental scan rate data.

The cyclic voltammetric shape ($E_p - E_{p/2}$) and peak potential for oxidation of electrogenerated $[Mn(CO)_5]^-$ (process II, Figure 2a) were also studied as a function of scan rate. This oxidation mechanism has been described as a one-electron-transfer step followed by a dimerization reaction,[4] and the data in CH_2Cl_2 are partially consistent with this mechanism. Theoretical equations that describe cyclic voltammetric curves for an electrochemically generated dimerization reaction have been presented independently by Savéant[36] and Nicholson.[37] A theoretical shift of 19.6 mV/10-fold increase in scan rate is predicted for reaction 6.

$$[Mn(CO)_5]^- \overset{-e^-}{\rightleftharpoons} Mn(CO)_5 \qquad (6a)$$

$$Mn(CO)_5 \rightarrow {}^1/_2Mn_2(CO)_{10} \qquad (6b)$$

Experimental plots of $\Delta E_p/\Delta \log V$ give a slope of 22 mV over a range of scan rates between 0.05 and 0.4 V/s and are thus in good agreement with that predicted for eq 6. On the other hand, the theoretical value of $|E_p - E_{p/2}|$ is 42 mV for reaction 6, and at the slowest scan rates examined, a value of 55 ± 5 mV was obtained. This shape might be accounted for by the occurrence of another slow step prior to dimerization in CH_2Cl_2 or, alternatively, an irreversibility in the initial oxidation. However, neither of these explanations is consistent with the experimentally obtained $\Delta E_p/\Delta \log V$, nor is the peak shape consistent with the known reactivity of $Mn(CO)_5$.

Although no direct evidence for the electrochemical generation of $Mn(CO)_5$ has ever been presented, this species must be formed in the direct one-electron oxidation of $[Mn(CO)_5]^-$. The $Mn(CO)_5$ radical is extremely short lived, and rapid dimerization to give $Mn_2(CO)_{10}$ should occur in CH_2Cl_2. Rate constants for this dimerization (reaction 7) have been reported to be between 0.6

$$2Mn(CO)_5 \rightarrow Mn_2(CO)_{10} \qquad (7)$$

$\times 10^9$ M^{-1} s^{-1} in ethanol[31] and 2.0×10^9 M^{-1} s^{-1} in cyclohexane[14] so that the overall oxidation process II appears to involve the direct conversion of $[Mn(CO)_5]^-$ to $Mn_2(CO)_{10}$, as shown in eq 8.

$$2[Mn(CO)_5]^- \rightarrow Mn_2(CO)_{10} + 2e^- \qquad (8)$$

This was verified in the present study. An exhaustive controlled-potential reduction of $Mn_2(CO)_{10}$ was carried out, and cyclic voltammograms of the resulting solution were analyzed. One such voltammogram is shown in Figure 2b. On the basis of the resulting cyclic voltammogram one can conclude that exhaustive controlled-potential electrolysis of $Mn_2(CO)_{10}$ gives $[Mn(CO)_5]^-$, as shown in eq 1. However, side reactions may occur with the intermediates as well as the final reduction products generated from $Mn_2(CO)_{10}$. These include the homogeneous reaction of electrogenerated $[Mn(CO)_5]^-$ with unreduced $Mn_2(CO)_{10}$ to give trimetallic $[Mn_3(CO)_{14}]^-$ (as identified by IR spectroscopy[3]), as well as the reaction of the $Mn(CO)_5$ radical with CH_2Cl_2 to give $Mn(CO)_5Cl$ after $Cl^\bullet$ abstraction. This latter species is also electroreducible[12] and regenerates the starting $Mn(CO)_5$ radical. However, it should be noted that these side reactions do not result in significant generation of products other than $[Mn(CO)_5]^-$, as this was the only product observed in the cyclic voltammogram.

The formation of both $[Mn_3(CO)_{14}]^-$ and $Mn(CO)_5O_2$ will lead to a decrease in the global number of electrons transferred in the reduction of the initial dimer. A decrease in the theoretical value of n has been observed by Dessy[1] and Lemoine[3], and in the later study a coulometric measurement gave n values of 1.9 rather than the expected 2.0 electrons for eq 1.

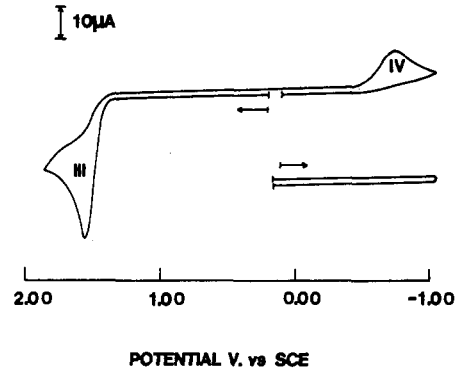

Figure 3. Cyclic voltammogram for the oxidation of $Mn_2(CO)_{10}$ at a Pt electrode in CH_2Cl_2 (0.1 M TBAP). Scan rate = 0.4 V/s.

As seen in Figure 2a, the maximum peak current for process II is significantly smaller than that for process I, but for the initial oxidation of $[Mn(CO)_5]^-$ (Figure 2b), the relative current heights are reversed. In theory, the ratio of anodic to cathodic peak currents should be close to unity if the potentials for the reactions are within 60–100 mV of each other and if there are no changes in the diffusion coefficients or concentrations of the oxidized or reduced species. This is not the case in the present study, which involves the reactions of both monomeric and dimeric species. However, in this study, the substantial differences in peak currents are mainly due to the large differences in peak potential between processes I and II (ΔE_p = 1.30 V). The electrogenerated species diffuse away from the electrode after electroreduction (or electrooxidation), and a much decreased concentration of electroactive species is present at the electrode surface during the return potential sweep of 1.3 V.

Similar voltammetric curves were observed for the reduction of $Mn_2(CO)_{10}$ in CH_2Cl_2, CH_3CN, and THF. Peak potentials of −1.32 V (CH_3CN) and −1.45 V (THF) were obtained for reaction 1 (process I) while the reoxidation of electrogenerated $[Mn(CO)_5]^-$ (reaction 2 and process II) occurred at E_{pa} = −0.06 V (THF) and −0.12 V (CH_3CN). The reduction peak shape was broad in THF and CH_3CN, similar to that observed in CH_2Cl_2, and transfer coefficients of 0.52 (THF) and 0.43 (CH_3CN) were calculated. At the same time, the oxidation peak shape was narrower (similar to that observed in CH_2Cl_2) and values of $|E_p - E_{p/2}|$ ranged between 59 and 64 mV (see Table II).

Electrochemistry of $Mn_2(CO)_{10}$ and $[Mn(CO)_5]^+$. The electrooxidation of $Mn_2(CO)_{10}$ generates $[Mn(CO)_5]^+$, as shown in eq 2. This species is stable in solution but can be reduced to $Mn(CO)_5$, which rapidly couples to regenerate the initial dimer (reaction 9). This EC mechanism for $[Mn(CO)_5]^+$ is similar to

$$[Mn(CO)_5]^+ \overset{e^-}{\rightleftharpoons} Mn(CO)_5 \qquad (9a)$$

$$Mn(CO)_5 \rightarrow {}^1/_2Mn_2(CO)_{10} \qquad (9b)$$

the EC mechanism given in eq 6 for $[Mn(CO)_5]^-$.

The electrooxidation of $Mn_2(CO)_{10}$ is characterized by a single oxidation peak or wave. This is shown by the rotating-disk voltammogram in CH_3CN (Figure 1) and the cyclic voltammogram in CH_2Cl_2 (Figure 3). This oxidation peak is labeled as process III. It is irreversible, and at a scan rate of 0.3 V/s the peak potential is located at E_p = 1.55 V. A similar irreversible oxidation peak is observed in CH_3CN, and at a scan rate of 0.2 V/s and the peak potential is E_p = 1.35 V vs. SCE. This negative potential shift upon changing solvents is consistent with a stabilization of the $Mn_2(CO)_{10}$ oxidation product(s) in CH_3CN.

The oxidation of $Mn_2(CO)_{10}$ is coupled to a reduction peak of electrogenerated $[Mn(CO)_5]^+$, and in Figure 3 this process occurs at an E_p = −0.76 V. This reduction (process IV) is not observed if the positive potential scan is terminated before the oxidation of $Mn_2(CO)_{10}$. In addition, the currents for the reduction process IV are substantially reduced in intensity with respect to those of the oxidation process III. This is similar to the case for the $Mn_2(CO)_{10}$ and $[Mn(CO)_5]^-$ currents and is not unexpected due

(36) Mastragostino, M.; Nadjo, L.; Savéant, J.-M. *Electrochim. Acta* **1968**, *13*, 721.
(37) Olmstead, M. L.; Hamilton, R. G.; Nicholson, R. S. *Anal. Chem.* **1969**, *41*, 260.

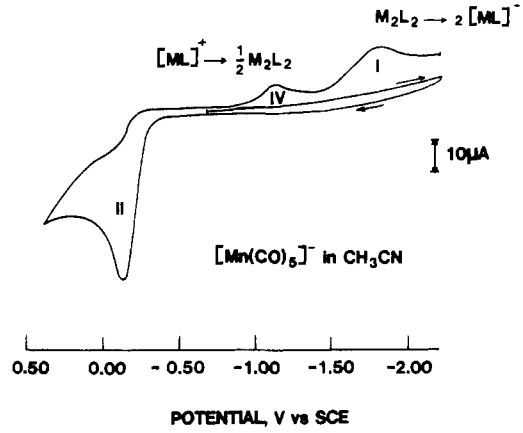

Figure 4. Cyclic voltammogram of $Na^+[Mn(CO)_5]^-$ at a Pt electrode in CH_3CN (0.1 M TBAP). Scan rate = 2.5 V/s. The relevant global electron-transfer processes are shown on the figure where M_2L_2 = $Mn_2(CO)_{10}$ and $[Mn(CO)_5]^-$ and $[Mn(CO)_5]^+$ are represented by $[ML]^-$ and $[ML]^+$, respectively.

to the large (2.25 V) potential separation between the two processes.

The potential for reduction of electrogenerated $[Mn(CO)_5]^+$ varies as a function of potential scan rate and the solvent system. At a scan rate of 0.2 V/s, $E_p = -0.76$ V in CH_2Cl_2 while in the more strongly bonding CH_3CN the measured E_p at this scan rate is −1.10 V. This negative shift of 0.34 V suggests a complexation of the electrogenerated cation with CH_3CN. This reaction is given by eq 10 and was first suggested by Pletcher.[4]

$$[Mn(CO)_5]^+ + CH_3CN \rightleftarrows [Mn(CO)_5(CH_3CN)]^+ \quad (10)$$

The peak shape for process III is characteristic of a diffusion-controlled one-electron-transfer process. Values of $|E_p - E_{p/2}| = 57 \pm 5$ mV were obtained from cyclic voltammograms in CH_2Cl_2 and CH_3CN. The oxidation of $Mn_2(CO)_{10}$ in CH_3CN at a rotating Pt-disk electrode is shown in Figure 1. Plots of log $(i/(i_d - i))$ vs. E were constructed and gave slopes of 62 ± 5 mV, which are consistent with an initial one-electron-transfer oxidation. However, the limiting current for the oxidation process at 1.33 V is identical with that for the two-electron reduction of $Mn_2(CO)_{10}$ at −1.41 V, thus indicating that the overall oxidation involves two electrons, as shown in eq 2. These combined data thus suggest an ECE mechanism as given in eq 11–13. The final

$$Mn_2(CO)_{10} \rightleftarrows [Mn_2(CO)_{10}]^+ + e^- \quad (11)$$

$$[Mn_2(CO)_{10}]^+ \rightarrow Mn(CO)_5 + [Mn(CO)_5]^+ \quad (12)$$

$$Mn(CO)_5 \rightleftarrows [Mn(CO)_5]^+ + e^- \quad (13)$$

product in the electrooxidation sequence is $[Mn(CO)_5]^+$, but in the presence of a bonding solvent such as CH_3CN, the cation should be converted to $[Mn(CO)_5(CH_3CN)]^+$.

A scan rate study was carried out in CH_2Cl_2 and showed that E_p for process III shifted positively along the potential axis with increase in scan rate. A plot of E_p vs. log V is linear and gives a slope of 28 ± 3 mV. This slope is consistent with that predicted for an EC mechanism where the first one-electron transfer is reversible and the following chemical reaction is irreversible.[32,33] Thus, the shape of the current voltage curves and the shift with scan rate are self-consistent with voltammetry at a rotating disk electrode and suggest the ECE mechanism shown by eq 11–13.

Formation of $[Mn(CO)_5]^+$ from $[Mn(CO)_5]^-$ in CH_3CN. The oxidation of $[Mn(CO)_5]^-$ has been described as proceeding via a one-electron-transfer step followed by a dimerization reaction.[4,38,39] While this mechanism appears to be accurate in a weakly coordinating solvent such as CH_2Cl_2, this does not appear to be the case in a stronger coordinating solvent such as CH_3CN.

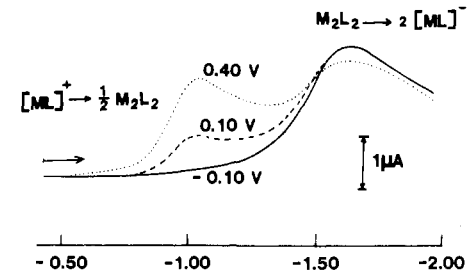

Figure 5. Linear-sweep voltammograms of $Na^+[Mn(CO)_5]^-$, which was first oxidized at a Pt microelectrode in CH_3CN for 30 s at (a) −0.10 V vs. SCE (—), (b) +0.1 V vs. SCE (- - -), and (c) +0.40 V vs. SCE (···) before potential scans were swept negatively from −0.40 V. The relevant global electron-transfer processes are shown on the figure.

Scheme I

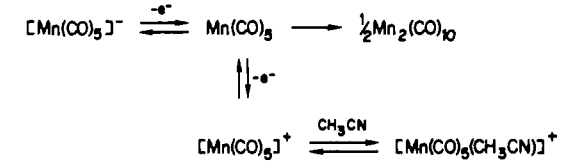

The two-electron oxidation of $[Mn(CO)_5]^-$ is illustrated by the cyclic voltammogram of $Na^+[Mn(CO)_5]^-$ in CH_3CN (Figure 4). Process II corresponds to the oxidation of $[Mn(CO)_5]^-$, which at a scan rate of 0.2 V/s occurs at $E_p = -0.12$ V (see Table I). This oxidation is coupled to two reverse reduction peaks located at $E_p = -1.10$ and −1.75 V. The peak at the more negative potential is due to reduction of $Mn_2(CO)_{10}$ (process I) and is shifted in a negative direction from that same process shown in Figure 2. This is due in part to the faster scan rate of 2.5 V/s but also to the fact that the electrode has become passivated under the given reaction conditions. On the other hand, the potential for the more positive (first) reduction is identical with that for reduction of $[Mn(CO)_5]^+$ in CH_3CN (process IV, Figure 3). *This suggests that $[Mn(CO)_5]^-$ can be directly converted to $[Mn(CO)_5]^+$ by a successive two-electron transfer in CH_3CN.* This type of reactivity has never been reported before and can be accounted for by Scheme I.

The potential at which controlled-potential oxidation of $[Mn(CO)_5]^-$ is performed influences the concentrations of $[Mn(CO)_5]^+$ produced; the larger the overpotential, the higher the $[Mn(CO)_5]^+$ concentration. This is shown in Figure 5, which illustrates linear-sweep voltammograms taken after $[Mn(CO)_5]^-$ was oxidized at increasingly more positive potentials for 30 s. If the oxidation is first performed for 30 s at a controlled potential of −0.10 V, only $Mn_2(CO)_{10}$ is produced (solid line, Figure 5a). In contrast, if the applied potential is held at +0.10 V for 30 s, a significant quantity of $[Mn(CO)_5]^+$ is formed. This is shown by the dashed line in Figure 5b. Finally, if the applied potential is held at 0.4 V for 30 s, $[Mn(CO)_5]^+$ becomes the major product (dotted line, Figure 5c). This increase in $[Mn(CO)_5]^+$ concentration can be explained by the fact that the rate of electron transfer between $Mn(CO)_5$ and $[Mn(CO)_5]^+$ is potential-dependent while that for dimerization of $Mn(CO)_5$ is potential-independent. Thus, the more positive the potential, the faster the rate of the second electron abstraction.

Currents for the $Mn_2(CO)_{10}$ reduction peak (process I) remain approximately constant at all three applied potentials since $Mn_2(CO)_{10}$ is the ultimate product generated from both process II and process IV. Thus, its concentration at the electrode surface will be invariant upon reaching reducing potentials more negative than −1.30 V. In this regard, it should be noted that the maximum

(38) Giraudeau, A.; Lemoine, P.; Gross, M.; Braunstein, P. *J. Organomet. Chem.* **1980**, *202*, 455.
(39) Lemoine, P.; Giraudeau, A.; Gross, M.; Braunstein, P. *J. Chem. Soc., Chem. Commun.* **1980**, 77.
(40) Hallock, S. A.; Wojcicki, A. *J. Organomet. Chem.* **1973**, *54*, C27.
(41) Kwan, C. L.; Kochi, J. K. *J. Organomet. Chem.* **1975**, *101*, C9.

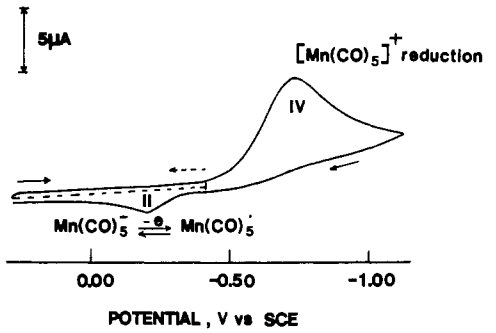

Figure 6. Cyclic voltammogram of $[Mn(CO)_5]^+$ in CH_2Cl_2 (0.1 M TBAP). The cationic species was generated from $Mn_2(CO)_{10}$ by controlled-potential oxidation at +1.55 V for 30 s. Scan rate = 0.4 V/s.

Scheme II

$$[Mn(CO)_5]^+ + e^- \rightleftharpoons Mn(CO)_5 \longrightarrow \tfrac{1}{2}Mn_2(CO)_{10}$$
$$\updownarrow +e^-$$
$$[Mn(CO)_5]^-$$

currents for $[Mn(CO)_5]^+$ reduction are approximately the same as the maximum currents for $Mn_2(CO)_{10}$ reduction, and this suggests that the majority of $Mn_2(CO)_{10}$ is generated at the electrode surface from $[Mn(CO)_5]^+$. Therefore, one must assume that under these conditions the predominant reaction in the oxidation of $[Mn(CO)_5]^-$ at 0.4 V is given by eq 14.

$$[Mn(CO)_5]^- \rightarrow [Mn(CO)_5(CH_3CN)]^- + 2e^- \quad (14)$$

Formation of $[Mn(CO)_5]^-$ from $[Mn(CO)_5]^+$. The reduction of $[Mn(CO)_5]^+$ in CH_2Cl_2 leads principally to $Mn_2(CO)_{10}$, as shown in eq 9. However, reduction of $[Mn(CO)_5]^+$ to $[Mn(CO)_5]^-$ is also possible before dimerization of the $Mn(CO)_5$ radical. This is shown by the mechanism in Scheme II. This scheme is very similar to Scheme I and involves the key point that *$[Mn(CO)_5]^+$ can be converted to $[Mn(CO)_5]^-$ by a two-electron oxidation.* In this regard it is important to note that the $Mn(CO)_5/[Mn(CO)_5]^-$ couple occurs at a more positive potential than the $[Mn(CO)_5]^+/Mn(CO)_5$ couple. This is most likely due to the kinetic factors that dominate the thermodynamics of the first reaction. There are numerous precedents in the literature for this effect.

Evidence for $[Mn(CO)_5]^-$ formation comes from cyclic voltammograms of $[Mn(CO)_5]^+$. This species was electrogenerated in CH_2Cl_2 by a controlled-potential oxidation of $Mn_2(CO)_{10}$ that was carried out for 30 s at 1.55 V with a Pt microelectrode. The potential was then switched to −0.40 V, from which cyclic potential scans were initiated. These scans are shown in Figure 6. As seen in this figure, a positive scan from −0.40 to +0.30 V gives no oxidation currents, but an oxidation peak at $E_p = -0.19$ V is observed after reduction of $[Mn(CO)_5]^+$ at $E_p = -0.76$ V. This oxidation peak potential is identical with that for process II in Figure 2 and thus is assigned as due to the $[Mn(CO)_5]^-/Mn(CO)_5$ reaction.

Overall Oxidation–Reduction Mechanism of $Mn_2(CO)_{10}$ and Related Species. The overall oxidation–reduction of $Mn_2(CO)_{10}$ is illustrated by the cyclic voltammogram in Figure 7. Basically, four electrode reactions are involved. These reactions are given by eq 1, 2, 6, and 9 and are labeled processes I, III, II, and IV, respectively.

All four peaks in Figure 7 are interrelated, and the four oxidation/reduction reactions give a reversible cyclical process. The initial $Mn_2(CO)_{10}$ is oxidized to $[Mn(CO)_5]^+$ at $E_p = 1.35$ V (peak III), and this species is reduced to $Mn_2(CO)_{10}$ at $E_p = -1.10$ V (peak IV) before reduction to $[Mn(CO)_5]^-$ at $E_p = -1.45$ V (peak I). Finally, the cyclical process is complete at $E_p = -0.12$ V where $[Mn(CO)_5]^-$ is oxidized to generate the original $Mn_2(CO)_{10}$ (peak II). A similar sequence is observed in both CH_2Cl_2 and THF,

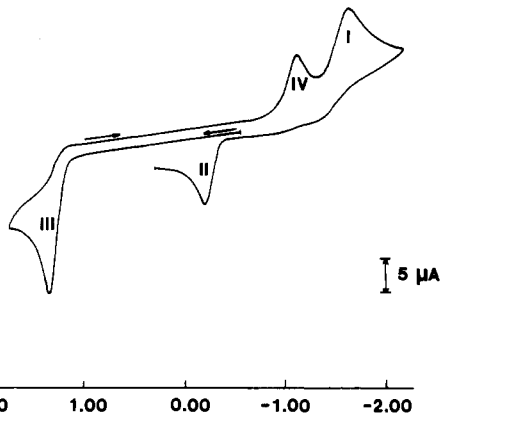

Figure 7. Cyclic voltammogram of $Mn_2(CO)_{10}$ that illustrates four of the relevant electron-transfer processes.

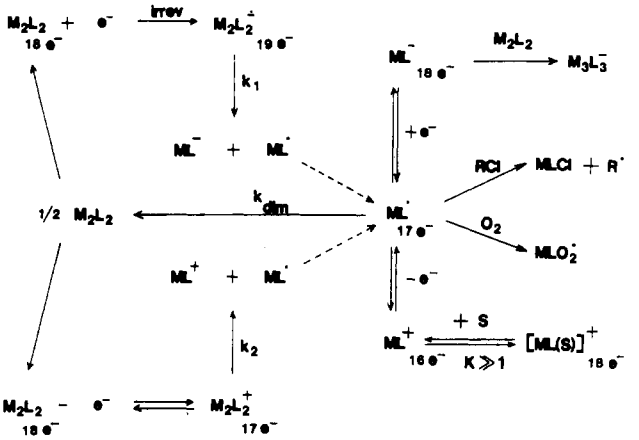

Figure 8. Overall mechanism for the electrochemical interconversion of $Mn_2(CO)_{10}$, $[Mn(CO)_5]^+$, $[Mn(CO)_5]^-$, and $Mn(CO)_5$. These species are represented by M_2L_2, $[ML]^+$, $[ML]^-$, and ML.

and the exact potentials for each of the four reactions in these solvents are given in Table I.

In conclusion, the overall electrochemical mechanism for the oxidation and reduction of $Mn_2(CO)_{10}$, as well as the oxidation of $[Mn(CO)_5]^-$ and the reduction of $[Mn(CO)_5]^+$, is presented in Figure 8. The key point in this mechanism is the presence of the $Mn(CO)_5$ radical. This species is formed by the oxidation or reduction of $Mn_2(CO)_{10}$ as well as by oxidation of $[Mn(CO)_5]^-$ or reduction of $[Mn(CO)_5]^+$. $Mn(CO)_5$ can also undergo numerous side reactions, such as reaction with halogenated solvents or reaction with O_2 to form $Mn(CO)_5O_2$.[17,18,31,42] Some of these possible side reactions are shown in Figure 8. The 17-electron $Mn(CO)_5$ species has been the object of many studies but has never been directly observed by electrochemical studies. However, a large body of data supports the existence and importance of this species as illustrated by the electrochemical study presented in this paper.

Acknowledgment. The support of the National Science Foundation (Grant CHE-8215507) is gratefully acknowledged. We also acknowledge several helpful conversations with Dr. Paul Lemoine, who read a preliminary draft of this paper.

Registry No. $Mn_2(CO)_{10}$, 10170-69-1; $[Mn(CO)_5]^+$, 71563-56-9; $[Mn(CO)_5]^-$, 14971-26-7; $Mn(CO)_5$, 15651-51-1; $[Mn_3(CO)_{14}]^-$, 45302-53-2; $Na^+[Mn(CO)_5]^-$, 13859-41-1.

(42) Fieldhouse, S. A.; Fullam, B. W.; Neilson, G. W.; Symons, M. C. R. *J. Chem. Soc., Dalton Trans.* **1974**, 567.
(43) Howard, J. A.; Morton, J. R.; Preston, K. F. *Chem. Phys. Lett.* **1981**, *83*, 226.